BJA

British Journal of Anaesthesia, 120 (5): 942–959 (2018)

doi: 10.1016/j.bja.2018.01.018
Advance Access Publication Date: 12 March 2018
Clinical Practice

Pharmacokinetic–pharmacodynamic model for propofol for broad application in anaesthesia and sedation

D. J. Eleveld[1,*], P. Colin[1,2], A. R. Absalom[1] and M. M. R. F. Struys[1,3]

[1]Department of Anesthesiology, University Medical Center Groningen, Groningen, The Netherlands, [2]Department of Bioanalysis, Faculty of Pharmaceutical Sciences, Ghent University, Ghent, Belgium and [3]Department of Anesthesia and Peri-operative Medicine, Ghent University, Ghent, Belgium

*Corresponding author. E-mail: d.j.eleveld@umcg.nl

This article is accompanied by an editorial: Increasing the utility of target-controlled infusions: one model to rule them all by Short, Campbell & Egan, *Br J Anesth* 2018:120:887–890, doi: 10.1016/j.bja.2018.02.012.

Background: Pharmacokinetic (PK) and pharmacodynamic (PD) models are used in target-controlled-infusion (TCI) systems to determine the optimal drug administration to achieve a desired target concentration in a central or effect-site compartment. Our aim was to develop a PK–PD model for propofol that can predict the bispectral index (BIS) for a broad population, suitable for TCI applications.

Methods: Propofol PK data were obtained from 30 previously published studies, five of which also contained BIS observations. A PK–PD model was developed using NONMEM. Weight, age, post-menstrual age (PMA), height, sex, BMI, and presence/absence of concomitant anaesthetic drugs were explored as covariates. The predictive performance was measured across young children, children, adults, elderly, and high-BMI individuals, and in simulated TCI applications.

Results: Overall, 15 433 propofol concentration and 28 639 BIS observations from 1033 individuals (672 males and 361 females) were analysed. The age range was from 27 weeks PMA to 88 yr, and the weight range was 0.68–160 kg. The final model uses age, PMA, weight, height, sex, and presence/absence of concomitant anaesthetic drugs as covariates. A 35-yr-old, 170 cm, 70 kg male (without concomitant anaesthetic drugs) has a V_1, V_2, V_3, CL, Q_2, Q_3, and k_{e0} of 6.28, 25.5, 273 litres, 1.79, 1.75, 1.11 litres min^{-1}, and 0.146 min^{-1}, respectively. The propofol TCI administration using the model matches well with recommendations for all age groups considered for both anaesthesia and sedation.

Conclusions: We developed a PK–PD model to predict the propofol concentrations and BIS for broad, diverse population. This should be useful for TCI in anaesthesia and sedation.

Keywords: propofol; pharmacokinetics; pharmacology

Editorial decision: January 22, 2018; **Accepted:** January 22, 2018

Editor's key points

- A new propofol pharmacokinetic–pharmacodynamic (PK–PD) model was developed using bispectral index (BIS) as the targeted endpoint based on previously published data from 30 studies.
- The PK–PD model predicted propofol concentrations and BIS for a diverse population, from neonates to the elderly and high-BMI individuals, for both anaesthesia and sedation.
- The model should likely be useful for target-controlled infusion in anaesthesia and sedation in population including a wide ranges of age and body weight.

Over the past three decades, numerous publications have described pharmacokinetic (PK) and pharmacodynamic (PD) models for predicting the time course of plasma and effect-site concentrations, and the relationship between concentration and effect of propofol, for numerous patient populations. Some of these models have been incorporated into infusion pumps and advisory displays[1] to guide propofol dosing and administration.[2–4] An important application of these models is target-controlled-infusion (TCI) systems that optimise propofol administration to achieve stable drug concentrations in plasma or an effect site associated with a clinically relevant drug effect rapidly. These systems are used in routine clinical practice and might play a beneficial role in patient outcomes.

TCI systems rely on PK and PD models that are most reliable when used in patients with similar characteristics to those of the study population. Thus, clinicians must be aware of the demographic support of the models they utilise, and might have to switch models when caring for different patient populations (e.g. children, adults, and obese patients). We previously showed[5] that analysing data (PK only) from multiple studies and estimating a single model can result in more accurate covariate detection and better performance across groups with diverse ages and weights even when compared with specialised models with narrow covariate ranges. Similar results have been obtained for remifentanil.[6,7] The single-model approach can also reduce uncertainty with regard to an appropriate TCI model[8] for a given clinical situation. There is no published PK–PD model for propofol with broad support for diverse age and weight groups.

Our aim was to develop a PK–PD model for propofol with broad support, achieving good predictive performance balanced across diverse subgroups, over a wide range of age and size, from neonates to the elderly, and both obese and non-obese individuals. Estimating a PD model enables its use in effect-site targeted TCI applications, whereas our previous propofol PK model only enabled plasma-targeted TCI. In addition, propofol PK was analysed focusing on physiologically relevant covariates, avoiding the patient/volunteer distinction of our previous general-purpose propofol PK model.[5] With the final model, we compare propofol dosing for use in TCI applications targeting anaesthesia and sedation with dosing recommendations from the official propofol drug label. If these are similar, this suggests that the TCI application of the model with appropriate targets results in adequate anaesthetic and sedative depth, as recommended in the propofol dosing guidelines. For comparison, we performed similar simulations of TCI using other PK–PD models used in commercial TCI systems.

Methods

For the PK model development, we applied previously published PK data[5] that were used for the development of a general-purpose PK model for propofol. We expanded these with data from propofol PK–PD studies where bispectral index (BIS) (Medtronic, Dublin, Ireland) data were available. In total, data from 30 studies (Table 1) was used. All included studies obtained the necessary ethical committee approval, as declared in the original publications or by the contributing authors.

From the available covariates, (postnatal) age, postmenstrual age (PMA), weight, height, sex, BMI, use of concomitant opioids or local anaesthetic drugs, and blood sampling site (arterial *vs* venous) were considered for potential relationships with model parameters. If PMA was not recorded, it was assumed to be 40 weeks longer than age. For some individuals, height was not recorded, so we assumed height was the average of other individuals of the same gender with weight within 5% of that of the individual with missing height data.

NONMEM version 7.3 (ICON Development Solutions, Ellicott City, MD, USA) was used for model estimation and evaluation using the first-order conditional estimation method with interaction. For calculations of model predictive performance, we used R (version 2.14.1) (R Foundation for Statistical Computing).[9]

Some studies listed in Table 1 used TCI administration of propofol; this produces infusion profiles with frequent small changes in infusion rate, resulting in slow NONMEM execution. We combined sequential infusion records if they were separated by <1 s and infusion rates differed by <0.5 mg min^{-1}. The two records were merged with the summed dose over the combined duration, until no dosing records could be combined. After the model development was completed, we estimated the final PK model with the non-reduced dosing records, and determined whether the estimated parameters differed significantly.

PK and PD analysis

A three-compartment mammillary PK model was used with volumes V_1, V_2, and V_3; elimination clearance CL; and intercompartmental clearances Q_2 and Q_3. We assumed that the recorded propofol concentrations represent plasma concentrations, predicted by the concentration in the central compartment V_1. The residual error was additively distributed in the logarithm of the observed and predicted concentrations. For model development, we used a reference individual[10] (a 70 kg male, 35 yr of age, and 170 cm tall). The model parameters were assumed to be either log-normally distributed or constant across the population. We did not consider PK models more complex than the three-compartment models.

The first model tested scaled all parameters linearly with weight.[11] We explored allometric scaling for model parameters, a method related to Kleiber's law[12] with a theoretical foundation in biology.[13] The scaling exponents used were the

Table 1 Details of the component datasets.

Dataset	N	Sampling	Age (years)	Weight (kg)	Additional drugs	Publication	Source
Bailey et al.	30	Arterial	44–79	50–122	Alfentanil	Bailey JM, Mora CT, Shafer SL. Pharmacokinetics of propofol in adult patients undergoing coronary revascularization. Anesthesiology: The Journal of the American Society of Anesthesiologists. 1996 Jun 1;84(6):1288–97.	Open-TCI
Billard 1998 Propofol	51	Venous	29–69	40–89	Alfentanil	SFAR abstract 1998, poster R279	Open-TCI
Coetzee Validation	30	Arterial	21–58	42–83	Sufentanil	Coetzee JF, Glen JB, Boshoff L. Pharmacokinetic model selection for target controlled infusions of propofol assessment of three parameter sets. Anesthesiology: The Journal of the American Society of Anesthesiologists. 1995 Jun 1;82(6):1328–45.	Open-TCI
Doufas Induction Speed	18	Arterial	20–43	51–83		Doufas AG, Bakhshandeh M, Bjorksten AR, Shafer SL, Sessler DI. Induction speed is not a determinant of propofol pharmacodynamics. Anesthesiology: The Journal of the American Society of Anesthesiologists. 2004 Nov 1;101(5):1112–21.	Open-TCI
Doufas DeRamp	10	Arterial	26–44	45–83		Doufas AG, Morioka N, Mahgoub AN, Bjorksten AR, Shafer SL, Sessler DI. Automated responsiveness monitor to titrate propofol sedation. Anesthesia & Analgesia. 2009 Sep 1;109(3):778–86.	Open-TCI
Doufas Fixed Reduction	10	Arterial	21–44	57–82		See Doufas DeRamp	Open-TCI
Doufas Redhead	29	Arterial	19–39	50–99		Doufas AG, Orhan-Sungur M, Komatsu R, Lauber R, Akca O, Shafer SL, Sessler DI. Bispectral index dynamics during propofol hypnosis is similar in red-haired and dark-haired subjects. Anesthesia & Analgesia. 2013 Feb 1;116(2):319–26.	Open-TCI
Dyck et al.	59	Arterial	23–82	57–114		See Coetzee Validation	Open-TCI
Gepts et al.	16	Arterial	25–65	48–84	Locoregional	Gepts E, Camu F, Cockshott ID, Douglas EJ. Disposition of propofol administered as constant rate intravenous infusions in humans. Anesthesia and analgesia. 1987 Dec;66(12):1256–63.	Open-TCI
Kataria et al.	53	Venous	3–11	15–60	Fentanyl	Kataria BK, Ved SA, Nicodemus HF, Hoy GR, Lea D, Dubois MY, Mandema JW, Shafer SL. The pharmacokinetics of propofol in children using three different data analysis approaches. Anesthesiology. 1994 Jan;80(1):104–22.	Open-TCI
Schnider et al.	24	Arterial	25–81	44–123		Schnider TW, Minto CF, Gambus PL, Andresen C, Goodale DB, Shafer SL, Youngs EJ. The influence of method of administration and covariates on the pharmacokinetics of propofol in adult volunteers. Anesthesiology: The Journal of the American Society of Anesthesiologists. 1998 May 1;88(5):1170–82.	Open-TCI
Servin et al, (obese)	8	Arterial	25–66	97–160	N20fentanyl	Servin F, Farinotti R, Haberer JP, Desmonts JM. Propofol infusion for maintenance of anesthesia in morbidly obese patients receiving nitrous oxide. A clinical and pharmacokinetic study. Anesthesiology. 1993 Apr;78(4):657–65.	Open-TCI
Servin et al, (alcoholic)	30	Venous	19–72	51–97	Alfentanil	Servin FS, Bougeois B, Gomeni R, Mentré F, Farinotti R, Desmonts JM. Pharmacokinetics of propofol administered by target-controlled infusion to alcoholic patients. Anesthesiology: The Journal of the American Society of Anesthesiologists. 2003 Sep 1;99(3):576–85.	Open-TCI
Struys et al.	10	Arterial	22–48	51–86		Struys MM, Coppens MJ, De Neve N, Mortier EP, Doufas AG, Van Bocxlaer JF, Shafer SL. Influence of administration rate on propofol plasma–effect site equilibration. Anesthesiology: The Journal of the American Society of Anesthesiologists. 2007 Sep 1;107(3):386–96.	Open-TCI
Coppens et al.	28	Venous, BIS	3–11	15–54		Coppens MJ, Eleveld DJ, Proost JH, Marks LA, Van Bocxlaer JF, Vereecke H, Absalom AR, Struys MM. An evaluation of using population pharmacokinetic models to estimate pharmacodynamic parameters for propofol and bispectral index in children. Anesthesiology: The Journal of the American Society of Anesthesiologists. 2011 Jul 1;115(1):83–93.	(MMRF Struys)
Marsh et al.	37	Venous	2–17	12–54	Regional	Marsh BM, White M, Morton N, Kenny GN. Pharmacokinetic model driven infusion of propofol in children. BJA: British Journal of Anaesthesia. 1991 Jul 1;67(1):41–8.	(M White)

Continued

Table 1 Continued

Dataset	N	Sampling	Age (years)	Weight (kg)	Additional drugs	Publication	Source
Cortinez et al. (children)	41	Arterial	0–2	5–11	Sevoflurane	Sepulveda P, Cortinez LI, Saez C, Penna A, Solari S, Guerra I, Absalom AR. Performance evaluation of paediatric propofol pharmacokinetic models in healthy young children. British journal of anaesthesia. 2011 Oct 1;107(4):593–600.	(I Cortinez)
Cortinez et al. (obese)	19	Arterial	28–56	82–134	Remifentanil	Cortinez LI, Anderson BJ, Penna A, Olivares L, Munoz HR, Holford NH, Struys MM, Sepulveda P. Influence of obesity on propofol pharmacokinetics: derivation of a pharmacokinetic model. British journal of anaesthesia. 2010 Oct 1;105(4):448–56.	(I Cortinez)
Servin et al. (cirrhosis)	9	Arterial	24–56	50–96	Opioids	Servin F, Cockshott ID, Farinotti R, Haberer JP, Winckler C, Desmonts JM. Pharmacokinetics of propofol infusions in patients with cirrhosis. British Journal of Anaesthesia. 1990 Aug 1;65(2):177–83.	(I Glen)
Swinhoe et al.	41	Arterial	21–79	36–104	Alfentanil	Swinhoe CF, Peacock JE, Glen JB, Reilly CS. Evaluation of the predictive performance of a 'Diprifusor'TCI system. Anaesthesia. 1998 Apr 1;53(s1):61–7.	(I Glen)
White et al.	107	Venous	17–88	42–100	Alfentanil	White M, Kenny GN, Schraag S. Use of target controlled infusion to derive age and gender covariates for propofol clearance. Clinical pharmacokinetics. 2008 Feb 1;47(2):119–27.	(M White)
Sahinovic et al.	40	Arterial, BIS	23–74	51–114		Sahinovic MM, Beese U, Heeremans EH, Kalmar A, van Amsterdam K, Steenbakkers RJ, Kuiper H, Spanjersberg R, Groen RJ, Struys MM, Absalom AR. Bispectral index values and propofol concentrations at loss and return of consciousness in patients with frontal brain tumours and control patients. British journal of anaesthesia. 2014 Jan 1;112(1):110–7.	(M.Sahinovic)
Colin et al.	20	Arterial, BIS	20–50	50–106		Colin P, Eleveld DJ, van den Berg JP, Vereecke HE, Struys MM, Schelling G, Apfel CC, Hornuss C. Propofol breath monitoring as a potential tool to improve the prediction of intraoperative plasma concentrations. Clinical pharmacokinetics. 2016 Jul 1;55(7):849–59.	(C. Hornuss)
Index of Consciousness	15	Arterial, BIS	23–66	50–95		ISAP abstract 17 at https://www.isaponline.org/events/past-annual-meetings/2013-annual-meeting/2013-annual-meeting-abstracts	(MMRF Struys)
Cortinez et al. (obese)	20	Arterial, BIS	21–53	77–141	Remifentanil	Cortínez LI, De la Fuente N, Eleveld DJ, Oliveros A, Crovari F, Sepulveda P, Ibacache M, Solari S. Performance of propofol target-controlled infusion models in the obese: pharmacokinetic and pharmacodynamic analysis. Anesthesia & Analgesia. 2014 Aug 1;119(2):302–10.	(I Cortinez)
Allegaert et al.	25	Arterial	0–0.07	0.68–4	Opioids	Allegaert K, Peeters MY, Verbesselt R, Tibboel D, Naulaers G, De Hoon JN, Knibbe CA. Inter-individual variability in propofol pharmacokinetics in preterm and term neonates. British journal of anaesthesia. 2007 Dec 1;99(6):864–70.	(K Allegaert)
Blussé van Oud-Alblas	14	Arterial	10–20	37–82	Remifentanil		(H.J. Blussé van Oud-Alblas)
Przbylowski (cancer)	23	Arterial	51–75	44–125	Some remifentanil	Przybyłowski K, Tyczka J, Szczesny D, Bienert A, Wiczling P, Kut K, Plenzler E, Kaliszan R, Grześkowiak E. Pharmacokinetics and pharmacodynamics of propofol in cancer patients undergoing major lung surgery. Journal of pharmacokinetics and pharmacodynamics. 2015 Apr 1;42(2):111–22.	(P Wiczling)
Kuizenga and colleagues (neural inertia)	72	Arterial	20–70	48–104	Some opoids	Kuizenga MH, Colin PJ, Reyntjens KM, Touw DJ, Nalbat H, Knotnerus FH, Vereecke HE, Struys MM. Test of neural inertia in humans during general anaesthesia. British Journal of Anaesthesia. 2017 Dec 13.	(MMRF Struys)
van den Berg and colleagues (adaptive TCI)	120	Arterial	44–75	46–114	Opoids	van den Berg JP, Eleveld DJ, De Smet T, van den Heerik AV, van Amsterdam K, Lichtenbelt BJ, Scheeren TW, Absalom AR, Struys MM. Influence of Bayesian optimization on the performance of propofol target-controlled infusion. British Journal of Anaesthesia. 2017 Nov 1;119(5):918–27.	(MMRF Struys)

Author name in brackets indicates personal communication.
Source: Open-TCI=http://www.opentci.org/ (downloaded on 11/13/2013).

theoretical values for PK models[14] that scale volumes to body size (usually weight) with a linear function and clearances to the power 0.75. Compartmental allometry[5,6] was also evaluated, where Q_2 and Q_3 scale to the estimated size of V_2 and V_3 in the individual, instead of to weight. Fat-free mass (FFM) was also considered as a compartment size descriptor using the Al-Sallami and colleagues[15] equation that uses weight (WGT, kg), age (AGE, yrs), BMI, and sex:

$$f_{\text{Al-Sallami and colleagues}} = \begin{cases} \left[0.88 + \dfrac{1-0.88}{1+(\text{AGE}/13.4)^{-12.7}}\right] \cdot \left[\dfrac{9270 \cdot \text{WGT}}{6680 + 216 \cdot \text{BMI}}\right], & \text{males} \\ \left[1.11 + \dfrac{1-1.11}{1+(\text{AGE}/7.1)^{-1.1}}\right] \cdot \left[\dfrac{9270 \cdot \text{WGT}}{8780 + 244 \cdot \text{BMI}}\right], & \text{females} \end{cases}$$

The PD measure BIS was modelled using a sigmoidal E_{max} model driven by an effect compartment concentration C_e. The effect compartment was connected to the central compartment by a first-order rate constant (k_{e0}). The PD equations were:

$$\frac{dC_e}{dt} = k_{e0} \cdot (C - C_e)$$

$$\text{drug effect} = \frac{{C_e}^{\gamma}}{{C_{e50}}^{\gamma} + {C_e}^{\gamma}}$$

$$\text{BIS} = \text{BIS}_{\text{baseline}} \cdot (1 - \text{drug effect}) + \varepsilon$$

where C is the concentration in V_1, and drug effect corresponds to the fraction of the maximal drug effect achieved, varying between 0 and 1 (between 0% and 100%). C_{e50} is the C_e associated with 50% drug effect, $\text{BIS}_{\text{baseline}}$ is the BIS measure in the absence of drug effect, γ is the steepness of the concentration *vs* BIS relation, and ε represents additive residual error. Other levels of drug effect can be denoted, such as the drug effect of 0.1 (10%) may be referred to as C_{e10}. BIS signal processing delay was estimated from the data, with a fixed minimum of 15 s. No distinction was made between the various BIS monitor software versions used. During PD model estimation, individual PK parameters were fixed to those estimated from the PK model estimation, known as the sequential method.[16,17]

Individual variability η values obtained from NONMEM estimation were used to identify significant covariates that were subsequently tested for inclusion in the model. We required the corrected Akaike information criterion (AIC) to decrease at least 20 for inclusion of a parameter in the model, and also required improvement in predictive performance measured using the method described as follows. Model modifications that decreased or left unchanged the number of parameters only required a decrease in AIC.

For the final PK and PD models, likelihood profiles were generated for estimated model parameters. Uncertainty was expressed as upper and lower 99% confidence limits, estimated via spline interpolation of the likelihood profiles. These were determined by the increase/decrease in each parameter required to increase the NONMEM objective function by 6.63.

Performance error, bias, and precision

During the PK model development, we evaluated bias and precision using the logarithmic prediction-error measure:[18]

$$\text{LE}_{\text{PK}} = \log\left(\text{C}_{\text{observed}} / \text{C}_{\text{predicted}}\right)$$
$$\text{ALE}_{\text{PK}} = |\text{LE}_{\text{PK}}|$$

For comparison with other PK models, we used the more widely applied performance error[19] (PE_{PK}) and absolute performance error (APE_{PK}) as:

$$\text{PE}_{\text{PK}} = \left(\text{C}_{\text{observed}} - \text{C}_{\text{predicted}}\right) / \text{C}_{\text{predicted}} \times 100\%$$
$$\text{APE}_{\text{PK}} = |\text{PE}_{\text{PK}}|$$

For BIS observations, we used performance error calculations more suitable for additive error models:

$$\text{PE}_{\text{BIS}} = \text{BIS}_{\text{observed}} - \text{BIS}_{\text{predicted}}$$
$$\text{APE}_{\text{BIS}} = |\text{PE}_{\text{BIS}}|$$

The LE and PE measures indicate bias, and the ALE and APE measures indicate precision. To summarise these, we report the median values, prefixing the measure with Md. We considered MdPE_{PK} <10–20% and MdAPE_{PK} of 20–40% to indicate clinically acceptable performance.[20,21] The performance error measures of the final model were compared with previously published propofol models: a general-purpose PK model we previously published,[5] adult models published by Schnider and colleagues,[22] Marsh and colleagues,[23] Cortínez and colleagues,[24] and White and colleagues,[25] and paediatric models published by Kataria and colleagues,[26] Short and colleagues,[27] Rigby-Jones and colleagues,[28] Rigby-Jones and colleagues (multicentre),[29] and the 'Paedfusor' model.[30,31]

Estimating PK predictive performance

At each step in model development, we estimated the ability of the model to predict out-of-sample observations (i.e. observations not included in the estimation data set). For this, we used repeated two-fold cross validation. Before analysis, individuals were randomly partitioned into equally sized groups: D1 and D2. The model was estimated using D1, and the parameters then held constant and used to predict D2 using only individual covariates (η fixed to 0). The process was then repeated, exchanging D1 and D2. Predictions for D1 and D2 were combined to obtain a complete set of predictions. To reduce sampling variability caused by random partitioning, this process was repeated twice, obtaining two predictions for every observation. This expanded set of predictions was used for measures of out-of-sample bias and precision.

To ensure that the model development was not dominated by the largest subgroup, we analysed five subgroups separately: young children (age <3 yr), children (3≤ age <18 yr),

non-obese adults (18≤ age <70 yr, BMI <30), elderly (age ≥70 yr), and high BMI (BMI ≥30). During PK model estimation, the average $MdALE_{PK}$ over these subgroups for the predictions/observations from repeated two-fold cross validation was interpreted as an overall measure of model predictive performance. For the PD model, we did the same with $MdAPE_{BIS}$. Better-performing models have a lower average $MdALE_{PK}$ and $MdAPE_{BIS}$ over the subgroups.

TCI simulations

With the final PK–PD model, we performed simulations of effect-site TCI and compared the resulting infusion profiles with propofol dosing recommendations and infusion profiles from other PK–PD models used in commercially available TCI systems. For the final PK–PD model with anaesthetic targets, we assumed the presence of concomitant anaesthetic techniques (e.g. opioids or local anaesthesia), whereas for sedation targets we assumed their absence. The simulated TCI propofol administered amounts and rates were compared with dosing recommendations from the propofol US Food and Drug Administration (FDA) approved drug product label[32] with the following dose recommendations for anaesthesia: children (3–16 yr) induction 2.5–3.5 mg kg^{-1} and maintenance 12–18 mg kg^{-1} h^{-1} for the first 30 min followed by 7.5–9 mg kg^{-1} h^{-1}; adults (18–55 yr) induction 2–2.5 mg kg^{-1} and maintenance 9–12 mg kg^{-1} h^{-1} for 15 min followed by a reduction of 40% (5.4–7.2 mg kg^{-1} h^{-1}) up to 30 min followed by 3–6 mg kg^{-1} h^{-1} afterwards; and elderly (age >55 yr) induction 1–1.5 mg kg^{-1} and maintenance 3–6 mg kg^{-1} h^{-1}. The dose recommendations for sedation were obtained from the same drug product label for monitored-anaesthesia-care (MAC) sedation: adults (18–55 yr) 6–9 mg kg^{-1} h^{-1} for 3–5 min (0.3–0.75 mg kg^{-1}), and then 1.5–4.5 mg kg^{-1} h^{-1} for 15 min followed by 1.5–3 mg kg^{-1} h^{-1}; and elderly (age >55 yr), 80% of the adult doses.

Anaesthesia targets in children, adults, and the elderly

Simulations of anaesthesia TCI for (non-obese) children, adults, and the elderly were performed using the final PK–PD model targeting an effect-site concentration equal to the age-adjusted C_{e50}. Children of 5-yr-old (18 kg and 109 cm) and 10-yr-old (32 kg and 139 cm) were simulated. Adults (35 and 70 yr) were assumed to have 70 kg weight and 170 cm height. We also performed TCI simulations using the PK–PD models incorporated into the Diprifusor[33] (plasma targeting) and by Schnider and colleagues[22] (effect-site targeting). For these models, only adults were simulated, and we used a target concentration of 4 μg ml^{-1}, which is the default concentration in the Diprifusor system.

Anaesthesia targets in obese adults

For simulation of anaesthesia TCI for obese adults, we assumed an age of 35 yr, height of 170 cm, and varied weight to achieve BMI values of 30–50. The target effect-site concentration was the same as for non-obese individuals, the age-adjusted C_{e50}. For the Diprifusor PK and Schnider and colleagues[22] PK–PD models, the target concentration was 4 μg ml^{-1}. The FDA drug product label for propofol does not specifically address drug dosing in obesity, so we adjusted adult (non-obese) recommendations by the equation of Servin and colleagues,[34] in which doses for obese individuals are based on ideal body weight (IBW) plus 40% of excess weight, where $IBW = 22 \cdot HGT^2$. Thus, the weight used for dosing was:

$$\text{dose weight (kg)} = \text{IBW} + 0.4(\text{WGT} - \text{IBW})$$

This approach serves to decrease dose per kilogram body weight in obese individuals as body weight exceeds IBW. Propofol administration from TCI simulations was compared with the adjusted dose recommendations.

MAC sedation in children, adults, and the elderly

To explore the TCI targeting sedation for children, adults, and the elderly, we performed simulations of TCI targeting the C_{e10} (i.e. 10% drug effect). This target was chosen subjectively because it would result in reduced drug effects and administration compared with anaesthesia. We compared drug administration with dosing recommendations for MAC sedation.

Results

In the PK analysis, there were 15 433 observations (11 530 arterial and 3903 venous) from 1033 individuals (672 males and 361 females) with an age range from 27 weeks PMA to 88 yr, and a weight range from 0.68 to 160 kg. For the defined subgroups, PK data from 71 young children, 128 children, 628 adults, 89 elderly, and 121 high-BMI individuals were analysed. For the PD analysis, there were 28 639 BIS observations from 122 individuals (56 males and 66 females) with an age range from 3 to 74 yr and a weight range from 15 to 141 kg. For the defined subgroups, PD data from 28 young children, 64 adults (including elderly), and 30 high-BMI individuals were analysed. The PK and PD observations are shown in Figure 1, and demographic information is shown in Supplementary Figure S1. Height information was missing for 108 individuals, for whom the estimated height was used for FFM and BMI calculations.

PK model development

The PK model development process for the final model is shown in Supplementary Table S1, and a detailed explanation of the steps in PK model building is included in Appendix 1. Briefly, the model incorporates allometric scaling, compartmental allometry, and a maturation model[35] for CL based on PMA. Peripheral volume V_2 declines with age, and CL and V_3 decline with age only when concomitant anaesthetic drugs are used. Parameter V_1 scales to an E_{max} function with weight. In females, CL is higher, and a slow-maturation function influences Q_3 to increase with age whilst Q_2 decreases. Peripheral volume V_3 scales with FFM. The residual error varies across individuals. Some model parameters reflect arterial–venous differences. Estimating the final model using the non-reduced dosing records caused longer estimation times, but the final parameter estimates were within the $P<0.05$ confidence limits of the (reduced data) final PK model. The equations of the final model are:

$$f_{\text{ageing}}(x) = \exp\left(x \cdot \left(\text{AGE} - \text{AGE}_{\text{ref}}\right)\right)$$

$$f_{\text{sigmoid}}(\text{x}, \text{E50}, \lambda) = \frac{x^{\lambda}}{\left(x^{\lambda} + \text{E50}^{\lambda}\right)}$$

$$f_{\text{central}}(x) = f_{\text{sigmoid}}(x, \Theta_{12}, 1)$$

$$f_{\text{CLmaturation}} = f_{\text{sigmoid}}(\text{PMA}, \Theta_8, \Theta_9)$$

$$f_{\text{Q3maturation}} = f_{\text{sigmoid}}(\text{AGE} + 40\text{weeks}, \Theta_{14}, 1)$$

$$f_{opiates}(x) = \left\{ \begin{array}{ll} 1, & \text{absence of opiates} \\ \exp(x \cdot \text{AGE}), & \text{presence } of \text{ opiates} \end{array} \right\}$$

$$V1_{\text{arterial}}(\text{litre}) = \Theta_1 \cdot \frac{f_{\text{central}}(\text{WGT})}{f_{\text{central}}\left(\text{WGT}_{\text{ref}}\right)} \cdot \exp(\eta 1)$$

$$V1_{\text{venous}}(\text{litre}) = V1_{\text{arterial}} \cdot (1 + \Theta_{17} \cdot (1 - f_{\text{central}}(\text{WGT})))$$

$$V2(l) = \Theta_2 \cdot \frac{\text{WGT}}{\text{WGT}_{\text{ref}}} \cdot f_{\text{aging}}(\Theta_{10}) \cdot \exp(\eta 2)$$

$$V3(l) = \Theta_3 \cdot \frac{f_{\text{Al-Sallami and colleagues}}}{f_{\text{Al-Sallami and colleagues,ref}}} \cdot f_{\text{opiates}}(\Theta_{13}) \cdot \exp(\eta 3)$$

$$CL\left(\text{litre} \cdot \text{min}^{-1}\right) = \left\{ \begin{array}{ll} \Theta_4, & \text{male} \\ \Theta_{15}, & \text{female} \end{array} \right\} \cdot \left(\frac{\text{WGT}}{\text{WGT}_{\text{ref}}}\right)^{0.75} \cdot \frac{f_{CLmaturation}}{f_{CLmaturation,ref}} \cdot f_{\text{opiates}}(\Theta_{11}) \cdot \exp(\eta 4)$$

$$Q2_{\text{arterial}}\left(\text{litre} \cdot \text{min}^{-1}\right) = \Theta_5 \cdot \left(V2 \middle/ V2_{\text{ref}}\right)^{0.75} \cdot (1 + \Theta_{16} \cdot (1 - f_{\text{Q3maturation}})) \cdot \exp(\eta 5)$$

$$Q2_{\text{venous}}\left(\text{litre} \cdot \text{min}^{-1}\right) = Q2_{\text{arterial}} \cdot \Theta_{18}$$

$$Q3\left(\text{litre} \cdot \text{min}^{-1}\right) = \Theta_6 \cdot \left(V3 \middle/ V3_{\text{ref}}\right)^{0.75} \cdot \frac{f_{Q3maturation}}{f_{Q3maturation,ref}} \cdot \exp(\eta 6)$$

$$\ln(C_{\text{observed}}) = \ln\left(C_{\text{predicted}}\right) + \Theta_7 \cdot \varepsilon \cdot \exp(\eta 7)$$

The symbols Θ_1–Θ_{18} are estimated model parameters, and η_1–η_7 are random variables representing inter-individual variability. The estimated model parameters and their uncertainty are shown in Table 2. AGE, PMA, and WGT represent the age (yr), PMA (weeks), and weight (kg), respectively. Symbols with the subscript ref are calculated for the reference individual. The symbol ε represents residual observation error in the log domain with a variance fixed to 1. The model diagnostic plots, complete PK data set, NONMEM code for the final model, and likelihood profiles can be found in Figure 2, Supplementary Digital Content S1, Supplementary Digital Content S2, and Supplementary Figure S2, respectively. From the model diagnostic plots, there is some upward bias for very early samples. This is likely because of our model lacking front-end kinetics effects.[18,36] Some under-prediction for very late samples is also evident, but we were unable to reduce this without compromising the overall performance.

PK prediction-error comparison

The final PK model was compared with published propofol PK models, shown in Supplementary Table S2. For both estimated (in-sample) and cross-validated (out-of-sample) predictions, the final PK model performed better than, or very similarly to, previously published models. The predictive performance of the final model was judged as likely to be clinically acceptable for all subgroups.

PD model development

Only three individuals with PD data were >70 yr old, so these were combined with the adult subgroup. The models evaluated during PD model development are shown in Supplementary Table S3, and a detailed explanation of the steps in PD model building is included in Appendix 2. Briefly, C_{e50} was found to decrease with age, whilst delay was found to increase with age. The parameter k_{e0} was found to be higher when the PK samples were venous. Residual error varied across individuals, and an asymmetric PD curve was found to improve the model fit. The allometric scaling of k_{e0} improved the extrapolation properties of the model without significantly degrading the model fit. The summarised equations of the final models are:

$$C_{e50}\left(\mu\text{g ml}^{-1}\right) = \Theta_1 \cdot f_{aging}(\Theta_7) \cdot \exp(\eta 1)$$

$$k_{e0}\left(\text{min}^{-1}\right) = \left\{ \begin{array}{ll} \Theta_2, & \text{arterial PK} \\ \Theta_8, & \text{venous PK} \end{array} \right\} \cdot \left(\frac{WGT}{70}\right)^{-0.25} \cdot \exp(\eta 2)$$

$$\text{BIS}_{\text{baseline}} = \Theta_3$$

$$\gamma = \left\{ \begin{array}{ll} \Theta_4, & \text{for } C_e \le C_{e50} \\ \Theta_9, & \text{for } C_e > C_{e50} \end{array} \right\}$$

$$\text{BIS} = \text{BIS}_{\text{baseline}} \cdot \left(1 - \frac{{C_{e50}}^{\gamma}}{{C_{e50}}^{\gamma} + {C_e}^{\gamma}}\right) + \Theta_5 \cdot \varepsilon \cdot \exp(\eta 3)$$

$$\text{BIS}_{\text{delay}}(S) = 15 + \exp(\Theta_6 \cdot \text{AGE})$$

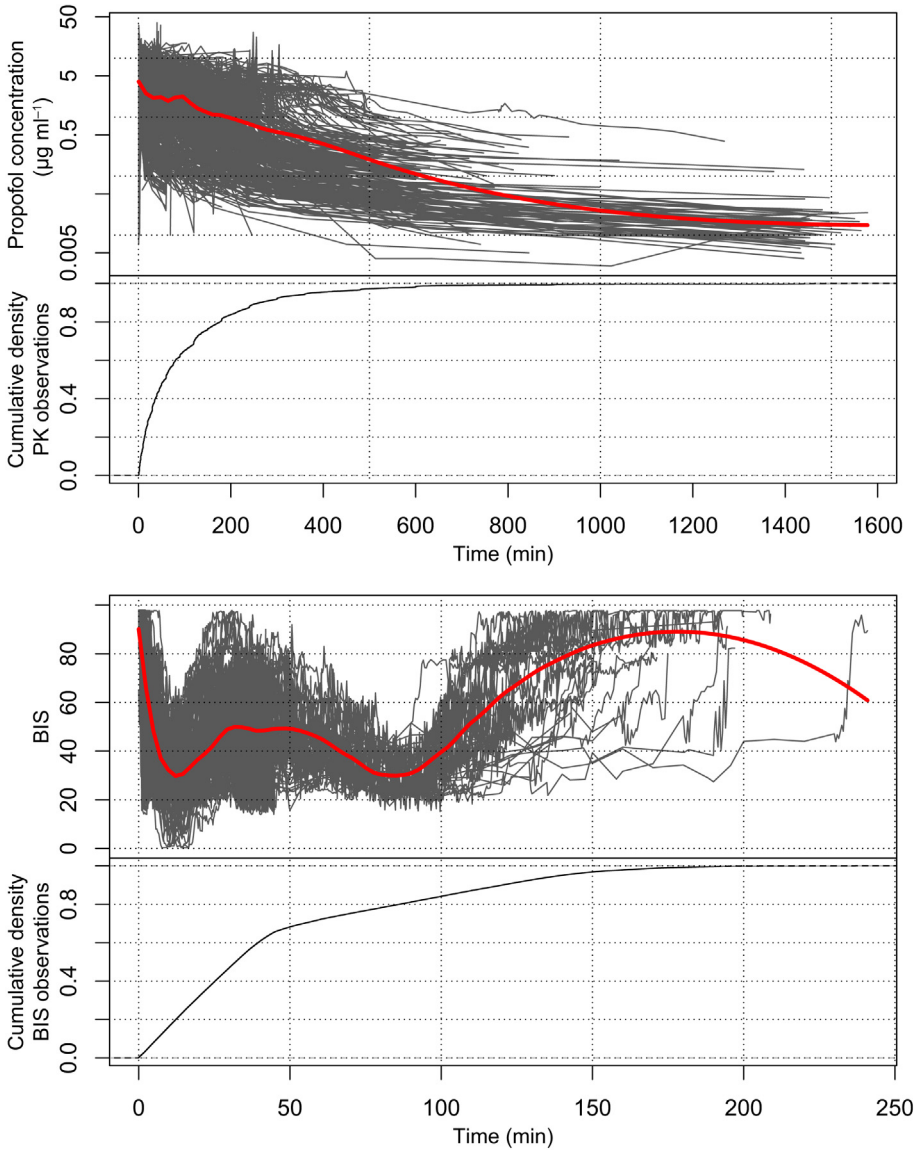

Fig 1. PK and PD observations analysed. The red line shows a Loess smoother. BIS, bispectral index; PD, pharmacodynamic; PK, pharmacokinetic.

The symbols Θ_1–Θ_9 represent the estimated model parameters, and η_1–η_3 are random variables representing inter-individual variability. The estimated parameter values are shown in Table 3. The symbol ε represents the additive residual observation error with a variance fixed to 1. The model diagnostic plots, complete PD data set, NONMEM code for the final model, and likelihood profiles can be found in Figure 3, Supplementary Digital Content S3, Supplementary Digital Content S4, and Supplementary Figure S4, respectively.

TCI simulations

For the final PK–PD model, the relationship between effect-site concentration and predicted BIS, and the relationship between age and effect-site concentration for 50% and 10% drug effect (C_{e50} and C_{e10}) are shown in Figure 4. For anaesthetic concentration targets, we assumed the presence of concomitant anaesthetic techniques (e.g. opioids or local anaesthesia), whereas for sedation targets we assumed their absence. For anaesthesia targets of the C_{e50}, the expected BIS value would be $93\cdot(1-0.5)=47$, whilst for MAC sedation targets of the C_{e10} it would be $93\cdot(1-0.1)=84$. Because C_{e50} and C_{e10} vary with age, the specific target concentration depends on age.

Anaesthesia targets in children, adults, and the elderly

Figure 5 shows the results from TCI simulations targeting the C_{e50} for (non-obese) children, adults, and elderly individuals using the final PK–PD model. Maintenance infusions are shown for illustrative individuals. The initial dose matches

Table 2 Final PK model estimated model parameters.

Parameter	Interpretation	Units	Estimated value	99% confidence limits	
				Lower	Upper
Θ_1	$V1_{ref}$	L	6.28	5.97	6.80
Θ_2	$V2_{ref}$	L	25.5	23.5	27.6
Θ_3	$V3_{ref}$	L	273	243	306
Θ_4	CL_{ref} *(male)*	$L \cdot min^{-1}$	1.79	1.71	1.87
Θ_5	$Q2_{ref}$	$L \cdot min^{-1}$	1.75	1.61	1.85
Θ_6	$Q3_{ref}$	$L \cdot min^{-1}$	1.11	1.02	1.20
Θ_7	Typical residual error		0.191	0.183	0.200
Θ_8	*CL* maturation E50	weeks	42.3	40.5	45.1
Θ_9	*CL* maturation slope		9.06	5.95	12.29
Θ_{10}	Smaller *V2* with age		−0.0156	−0.0185	−0.0128
Θ_{11}	Lower *CL* with age		−0.00286	−0.00388	−0.00186
Θ_{12}	Weight for 50% of maximal *V1*	Kg	33.6	22.8	50.0
Θ_{13}	Smaller *V3* with age		−0.0138	−0.0171	−0.0107
Θ_{14}	Maturation of *Q3*	weeks	68.3	52.4	86.0
Θ_{15}	CL_{ref} *(female)*	$L \cdot min^{-1}$	2.10	2.00	2.21
Θ_{16}	Higher *Q2* for maturation of Q3		1.30	0.70	2.13
Θ_{17}	*V1* venous samples (children)		1.42	0.92	1.78
Θ_{18}	Higher *Q2* venous samples		0.68	0.62	0.78

	Inter-individual variability	Variance (ω^2)	CV(%)
η_1	*V1*	0.610	91.7
η_2	*V2*	0.565	87.1
η_3	*V3*	0.597	90.4
η_4	*CL*	0.265	55.1
η_5	*Q2*	0.346	64.3
η_6	*Q3*	0.209	48.2
η_7	Residual error	0.463	76.7

The coefficient of variation is reported as: $CV(\%) = \sqrt{e^{\omega^2} - 1} \cdot 100\%$.

well with induction dosing recommendations (shaded areas) across a wide age range, with smooth interpolation across age ranges. The maintenance infusion rates are also within or close to recommendations.

Figure 6 shows the propofol administration with the Diprifusor PK and Schnider and colleagues[22] PK–PD models targeted to 4 μg ml^{-1}. For both models, induction doses are smaller than recommended for 18–55-yr-old individuals, but closer to recommendations in the elderly. The maintenance infusion rates are higher than recommended for young adults and the elderly. Both the Diprifusor and Schnider and colleagues[22] models require target adjustments depending on the patient group (young *vs* elderly) and over time (induction *vs* maintenance) for propofol administration to be close to recommendations.

Anaesthesia targets in obese adults

Figure 7 shows the results from the TCI simulations for obese (BMI >30) adults for the final PK–PD model. The propofol administration matches well with anaesthesia induction and maintenance dosing recommendations when these are corrected using the equation of Servin and colleagues.[34] Diprifusor initial doses are lower than recommended for BMI of ~30, and the dose (per kilogram) is not affected by changes in BMI. In contrast, the equation of Servin and colleagues[34] suggests that a lower (per kilogram body weight) initial dose is required as BMI increases into obesity. The maintenance infusion rates are higher than recommended in this group. The Schnider and colleagues[22] model yields lower than the recommended initial doses for obese individuals, <1 mg kg^{-1}, and higher than the recommended maintenance infusion rates. For this group, both the Diprifusor and Schnider and colleagues[22] models require target adjustments depending on the patient group (obese *vs* non-obese) and over time (anaesthesia *vs* maintenance) for propofol administration to match recommendations.

MAC sedation in children, adults, and the elderly

Figure 8 shows the results from the TCI simulations of the final PK–PD model targeting C_{e10} (i.e. effect-site concentrations associated with 10% drug effect). The initial dose and maintenance infusion rates correspond well with recommendations for MAC sedation.

Discussion

We developed a three-compartment PK model and effect-site sigmoidal PD model to predict propofol concentrations and BIS values for broad populations of individuals. The covariates of the PK model used to predict arterial concentrations were age, weight, height, and sex. PMA is also necessary for children younger than 5–6 months. Some parameters differ when concomitant anaesthetic drugs were used, such as opioids or local anaesthetics. The predictive performance of the PK model was good for all subgroups considered, and was generally better than that of previously published models. The covariates of the PD model were age and weight. Increasing age is associated with increased propofol sensitivity (decreased C_{e50}) and increased lag time of the BIS signal.

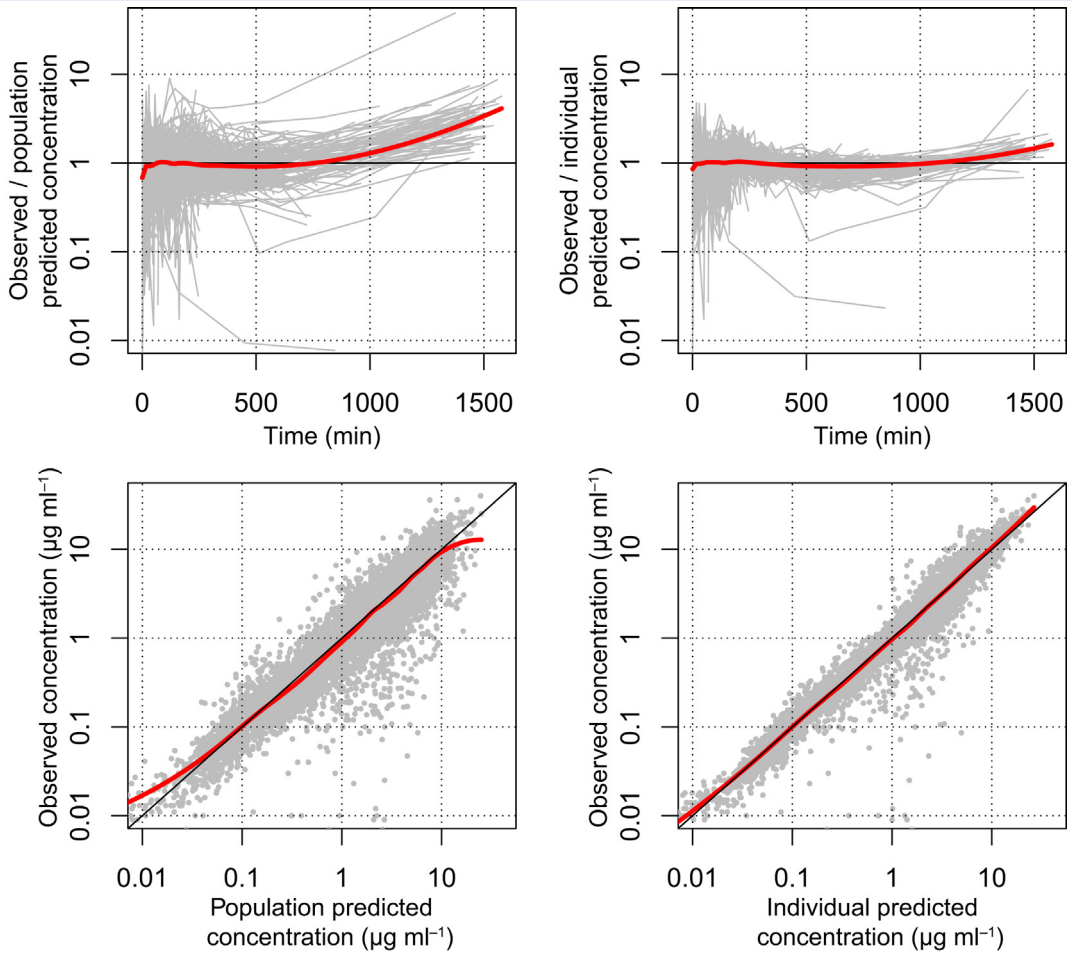

Fig 2. Population and individual PK predictions for the final PK model *vs* time and observed propofol concentration. The red line is a Loess smoother. PK, pharmacokinetic.

We found that, when targeting C_{e50}, the final PK–PD model results in propofol administration close to recommendations for anaesthesia in children, adults, and the elderly. The C_{e50} target would be expected to achieve a BIS value of 47, which is in the commonly clinically applied range of 40–60 for anaesthesia. For obese adults, the same C_{e50} target results in propofol administration matching recommendations for anaesthesia, provided these are adjusted according to the equation of Servin and colleagues.[34] In contrast, TCI using the Diprifusor or Schnider and colleagues[22] model requires target adjustments depending on the patient group (adult *vs* elderly and obese *vs* non-obese) and over time (induction *vs* maintenance) for propofol administration to be close to recommendations.

We showed that, when targeting C_{e10}, the final PK–PD model results in propofol administration close to recommendations for MAC sedation. However, the BIS predictions of the final model may be biased in this range, because none of the data used in the development of the PK–PD model were derived from studies targeting sedation.

The good agreement between propofol administration determined by the final PK–PD model and recommendations can be seen as validation of the PK–PD model. The dose recommendations were developed independently, but achieve presumably similar clinical results, namely, clinically adequate levels of anaesthesia or sedation. This concordance suggests that the PK–PD model will be clinically useful when targeted to clinically relevant drug-effect levels, because propofol administration amounts and rates remain in a range likely to be familiar to clinicians. Of course, inter-individual variability and diverse clinical conditions also influence the appropriate dose, and thus TCI targets as well. For example, cardiac patients are recommended to receive an induction dose of 0.5–1.5 mg kg^{-1}, which is considerably lower than for (non-cardiac) adults. Thus, with the current PK–PD model, targets lower than C_{e50} are necessary for propofol administration to be close to recommendations for cardiac patients.

Drug transport to the effect site

The estimated k_{e0} value of 0.146 min^{-1} for a 35-yr-old individual is considerably slower than the 0.456 min^{-1} of the Schnider and colleagues[22] model. A direct comparison of k_{e0} values is not really valid, because the specific value depends on the PK, and the PK of our model differs from that of the

Table 3 Final PD model estimated model parameters.

Parameter	Interpretation	Units	Estimated value	99% confidence limits	
				Lower	Upper
Θ_1	*Ce50*	$\mu g \cdot ml^{-1}$	3.08	2.91	3.26
Θ_2	*ke0* for arterial samples	min^{-1}	0.146	0.121	0.177
Θ_3	Baseline BIS value		93.0	92.3	93.7
Θ_4	PD sigmoid slope (*Ce*>*Ce50*)		1.47	1.44	1.51
Θ_5	Residual error	BIS	8.03	7.59	8.49
Θ_6	Increase in delay with age		0.0517	0.0499	0.0534
Θ_7	Decrease in *Ce50* with age		−0.00635	−0.00917	−0.00353
Θ_8	*ke0* for venous samples	min^{-1}	1.24	0.87	1.80
Θ_9	PD sigmoid slope (*Ce*<*Ce50*)		1.89	1.83	1.96

	Inter-individual variability	Variance (ω^2)	CV(%)
η_1	*Ce50*	0.242	52.3
η_2	*ke0*	0.702	101
η_3	Residual error	0.230	50.9

The coefficient of variation is reported as: $CV(\%) = \sqrt{e^{\omega^2} - 1} \cdot 100\%$.

Schnider and colleagues[22] model. Also, Schnider and colleagues[22] studied a different PD measure, the canonical univariate parameter, whilst we considered BIS. From the existing literature, the published k_{e0} values for BIS are similar to ours. Doufas and colleagues[37] estimated a k_{e0} of 0.17 min^{-1}, whilst Cortínez and colleagues[38] found 0.19 min^{-1}. Faster k_{e0} values have been estimated when venous sampling was used. Coppens and colleagues[39] estimated a value of 0.79 min^{-1} for

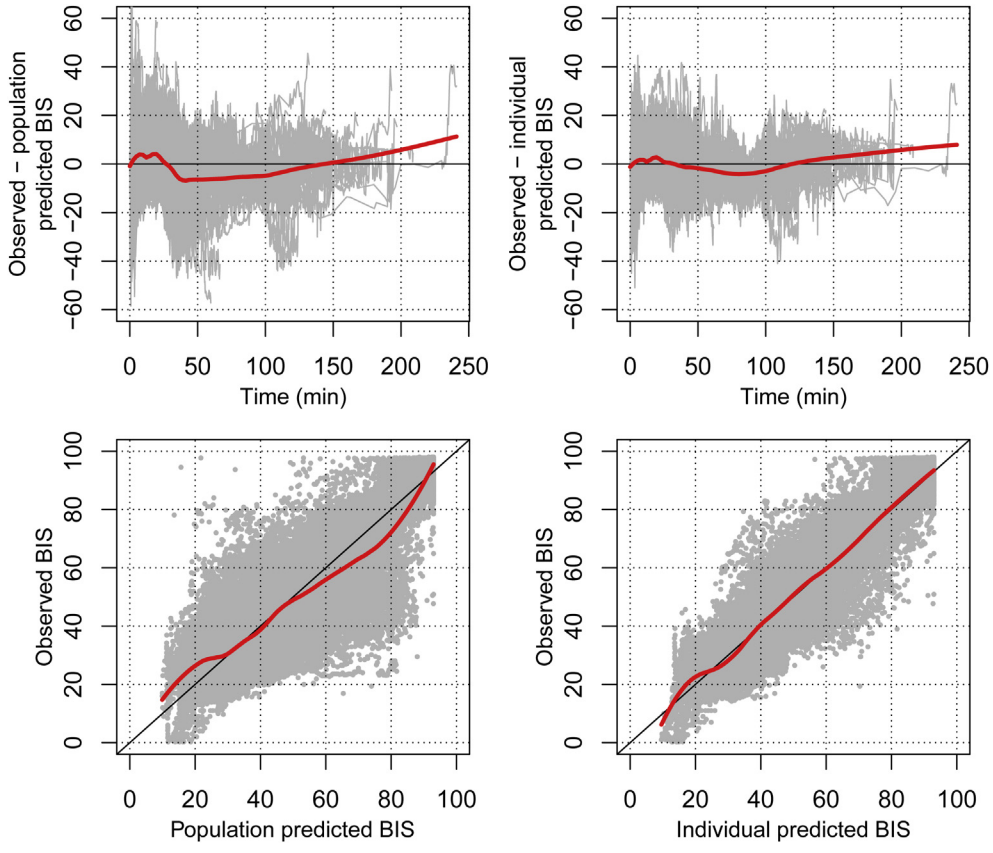

Fig 3. Population and individual PD predictions for the current study *vs* time and observed BIS. The red line is a Loess smoother. BIS, bispectral index.

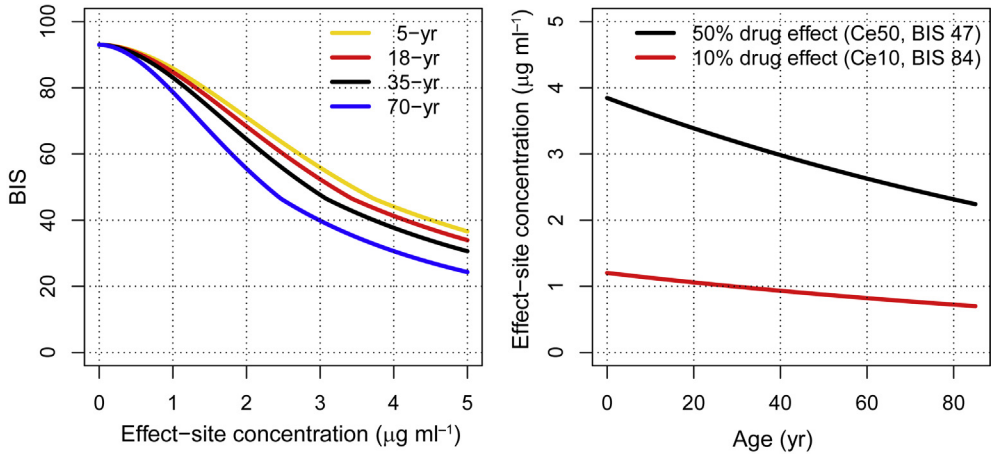

Fig 4. Relationships between effect-site concentration and predicted BIS, and the relationship between age and effect-site concentration for 50% and 10% drug effect for the final PK–PD model. BIS, bispectral index.

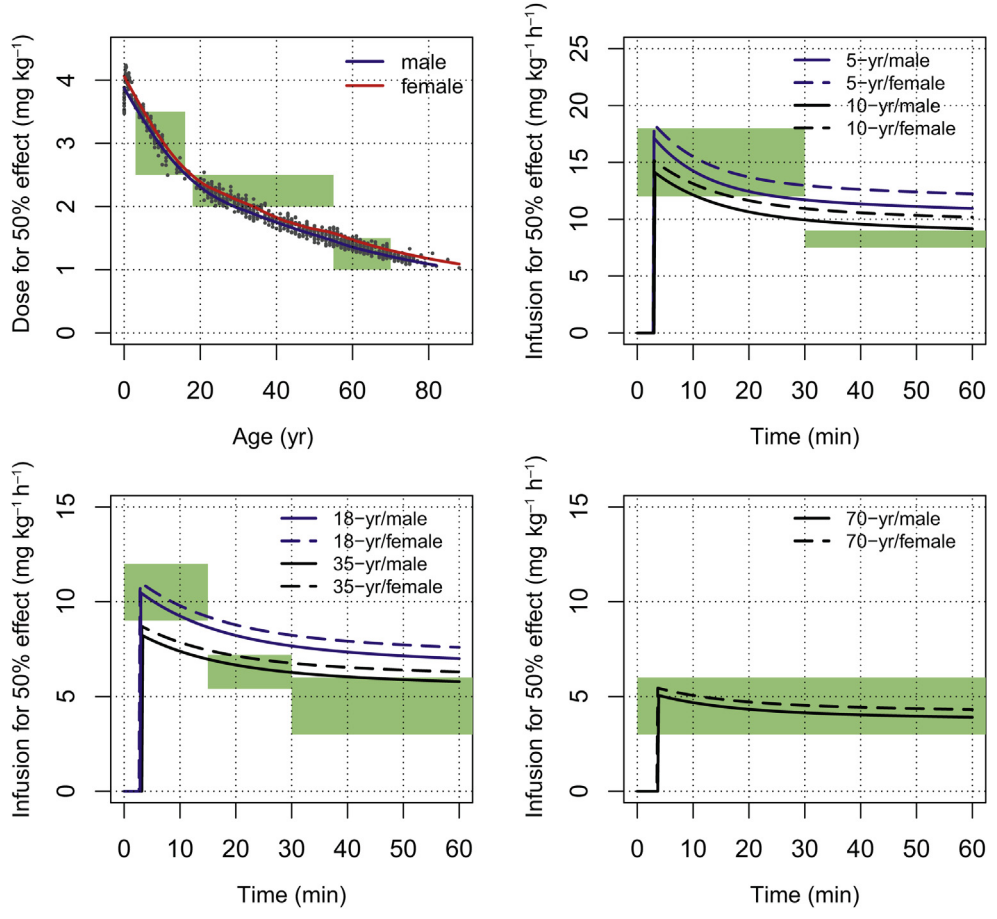

Fig 5. Predicted initial dose for 50% drug effect *vs* age for all of the individuals studied and maintenance infusion rates over time for illustrative children (5 yr, 18 kg, and 109 cm; 10 yr, 32 kg, 139 cm), adults (18 and 35 yr, 70 kg, and 170 cm), and elderly (70 yr, 70 kg, and 170 cm) individuals, assuming concomitant opioid administration. Induction and maintenance dosing recommendations for anaesthesia from the propofol package insert are shown in the green shaded areas. Both the initial dose and maintenance infusion rates are generally close to recommended with smooth interpolation across the age range.

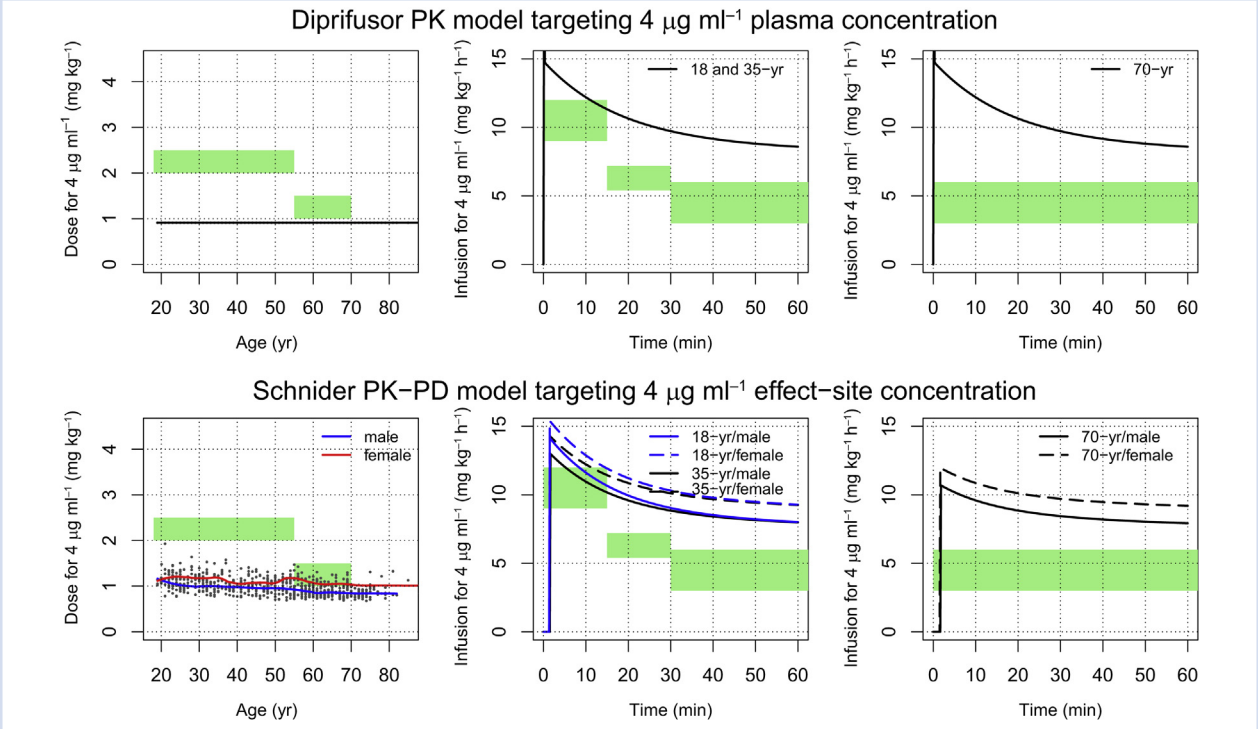

Fig 6. Predicted initial dose for all of the individuals studied and maintenance infusion rates targeting 4 μg ml^{-1} for illustrative adults (35 yr, 70 kg, and 170 cm) and elderly (70 yr, 70 kg, and 170 cm) individuals with the Diprifusor and Schnider and colleagues[22] models. Dose recommendations are shown in the green shaded areas. With the Diprifusor model, the initial drug administration is lower than the recommended induction for adults, but closer in the elderly. With the Schnider and colleagues[22] model, the initial doses are smaller than the recommended induction for adults, but similar in the elderly. For both models, the maintenance infusion rates are higher than the recommended in adults and the elderly. PD, pharmacodynamic; PK, pharmacokinetic.

children, and Chidambaran and colleagues[40] found a value of 0.61 min^{-1} for severely obese adolescents. When incorporating our model in a TCI algorithm, arterial concentrations should be used for both PK and k_{e0}.

Concomitant opioid administration

We found an association between age and opioid sensitivity, as elimination clearance CL and distribution volume V_3 decrease with age when concomitant anaesthetic adjuvant drugs were applied (e.g. opioids or local anaesthetics). For opioids, decreased liver blood flow caused by opioid-induced cardiovascular depression is a possible mechanism. Midazolam has been shown to reduce propofol CL and inter-compartmental clearances.[41] Propofol interaction studies show additivity with remifentanil,[42,43] which might be explained as reduced propofol CL and V_3 in the presence of opioids.

When concomitant anaesthetic adjuvant drugs are applied, the PK model only indicates their presence or absence. For opioids especially, it seems obvious that the applied dose and achieved concentrations would play a role in a more physiological model. Unfortunately, precise dosing information for these additional drugs is absent in the data we analysed, so we cannot construct a more detailed model at this time. With the current approach, the model may not perform ideally when opioid administration is substantially greater than in the studies considered. In this situation, lower propofol administration and lower degrees of hypnosis are likely appropriate to avoid excessive anaesthetic depth.[44] This can be achieved by lowering the effect-site concentration or drug-effect targets. Despite its simplicity, our current approach has a better physiological basis than the distinction between patients *vs* healthy volunteers used in the general-purpose PK model we developed previously.[5] The apparent difference in propofol PK between patients and volunteers might be explained by the lack of supplemental anaesthetic drug administration in healthy volunteer studies.

Maturation

We found that a maturation model for CL based on PMA was a beneficial component of the model. The biological processes underlying propofol clearance appear to be immature in very young/small individuals. The use of a sigmoidal function to represent maturation has been suggested.[14] Our results are slightly different than those reported by Allegaert and colleagues[45] in that our maturation function is steeper, and that maturation in CL is rapid around birth and 95% complete at 5 months of age. Both results clearly indicate that reduced CL should be expected around birth, with very low values for neonates. Our results suggest that, for children older than about 6 months, CL maturation is essentially complete.

Maturation of Q_3 appears to occur more slowly, requiring almost 11 yr for 90% maturation. Also, Q_2 decreases and Q_3

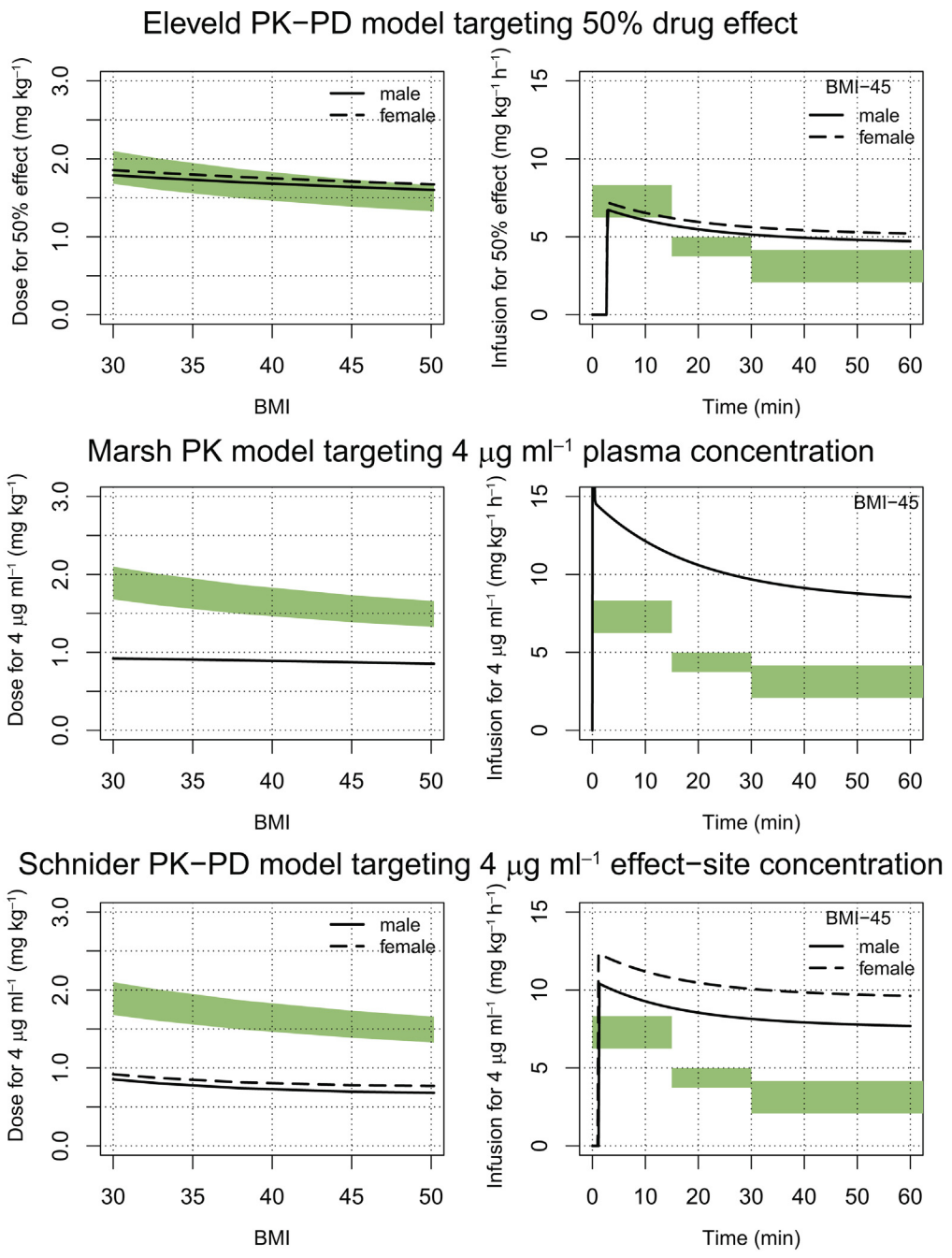

Fig 7. Predicted initial dose and maintenance infusions for obese individuals for the final PK–PD model targeting 50% drug effect, and for the Diprifusor and Schnider and colleagues[22] models targeting 4 μg ml^{-1}. Individuals had an age of 35 yr and height of 170 cm. The recommended propofol induction doses and maintenance infusion rates corrected by the equation of Servin and colleagues[34] are shown in the green shaded areas. For the final PK–PD model, the initial dose and maintenance infusion rates are generally close to the recommended, whereas the Diprifusor and Schnider and colleagues[22] models require corrections to concentration targets, varying with BMI and over time. PD, pharmacodynamic; PK, pharmacokinetic.

increases as maturation progresses. This might reflect changes during growth where total body water decreases as a percentage of FFM with age and percentage body fat increases rapidly in infancy, but slowly decreases into adolescence.[46]

Allometric scaling

We found that allometric scaling and compartmental allometry were beneficial for model performance, as was also found

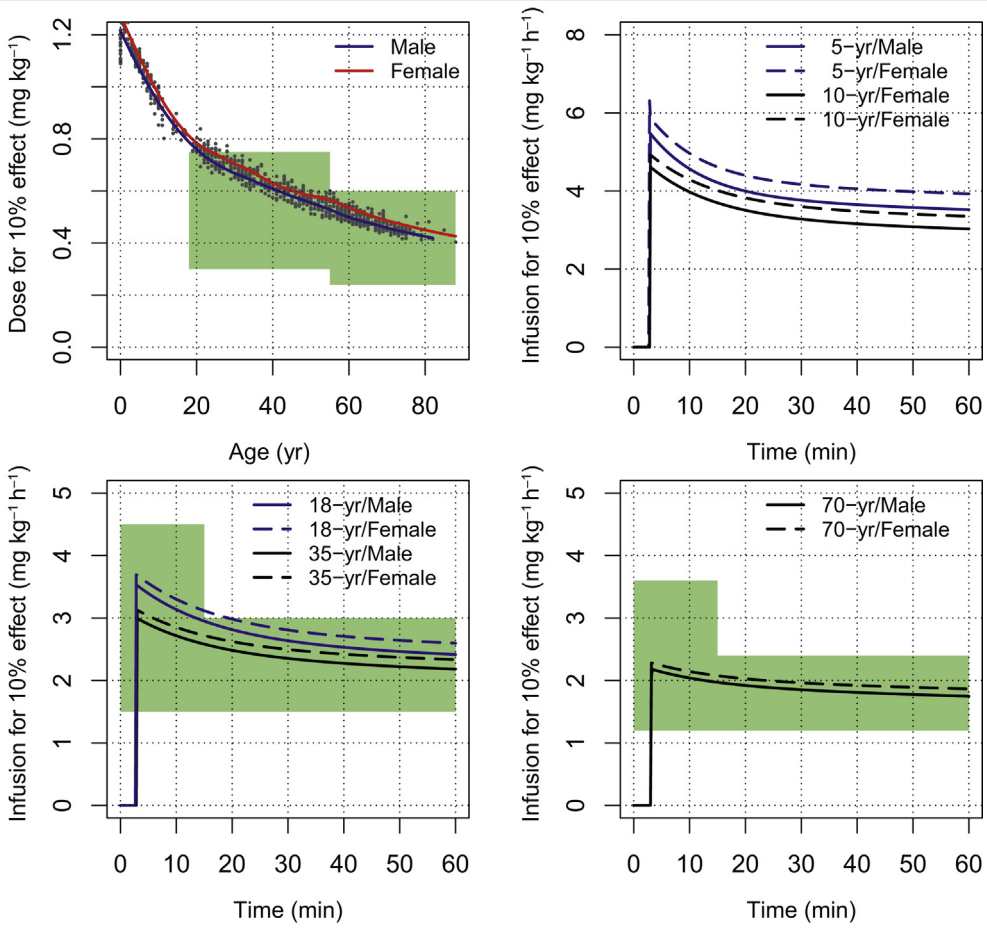

Fig 8. Predicted initial dose and maintenance infusion rates for the final PK–PD model targeting 10% drug effect for children (5 yr, 18 kg, 109 cm; and 10 yr, 32 kg, and 139 cm), adults (18 and 35 yr, 70 kg, and 170 cm), and elderly (70 yr, 70 kg, and 170 cm) individuals in the absence of concomitant anaesthetic techniques. Drug administration matches well with dose recommendations for sedation (green shaded areas). PD, pharmacodynamic; PK, pharmacokinetic.

for remifentanil.[6] This approach avoids the James lean-body-mass equation, which is used in the Schnider and colleagues[22] and other models, and avoids its paradoxical behaviour in obese individuals.[47]

Our PD model applies allometric scaling to k_{e0}, scaling it to $(WGT/70)^{-0.25}$. Whilst this has been considered before,[6,48] we found that it results in more reasonable model characteristics for children, even though it did not improve the model fit. Our approach was to choose the most useful model consistent with the data.

Drug-effect targeting

In the PD model, there is a one-to-one relationship between drug effect and BIS values. So, whilst we denote the C_{e50} for anaesthesia and C_{e10} for MAC sedation as TCI targets, these can equivalently be given as a percentage drug effect (50% or 10%) or as target BIS values (47 or 84). Allowing clinicians to target drug-effect percentages or BIS values directly may have clinical advantages. This approach can compensate automatically for the considerable non-linearity in propofol PD. Verifying this requires further study.

Limitations of the study

This study has several limitations. First, the PK–PD model was not prospectively evaluated; this should be done to evaluate its safety and efficacy. Second, for BIS observations, only one study in children was analysed, adolescents 12–19 yr are absent, and only three individuals older than 67 yr were analysed. Thus, the PD model has the weakest support in children and the elderly, and no support in young children and adolescents. Third, the three-compartment PK model shows some bias for late samples, indicating that terminal elimination is incorrectly modelled. Adding a fourth PK compartment could solve this problem, but we do not consider these models here. Fourth, during PK model development, we evaluated the predictive performance by averaging MdALE measures over subgroups. This measure might not be appropriate for every application. Fifth, the BIS signal has PK delays in the biophase in addition to processing and smoothing delays. Other clinically important PD responses, such as haemodynamic and respiratory changes, result from propofol actions on different systems and likely involve different lag times and rate constants. A propofol infusion profile optimal for BIS may not be optimal for other responses.

One could criticise our simulations of the Diprifusor and Schnider and colleagues[22] PK–PD models targeting 4 μg ml^{-1} as unrealistic, as in clinical practice, drug administration is 'titrated to effect' for each individual. This titration would also be necessary to individualise propofol administration when using the final PK–PD model. However, for the Diprifusor and Schnider and colleagues[22] models, we show that no single target results in propofol administration matching recommendations, and target adjustments are likely necessary depending on the patient's age or obesity and over time as well. These target adjustments are additional mental and physical workload for the clinician, increasing the risk of subjectivity and errors. It seems reasonable to expect that fewer target adjustments would be necessary with the final PK–PD model, because covariate adjustment and time-related factors seem better handled. However, this must be experimentally verified.

We created a PK–PD model for propofol with support from a diverse population, from neonates to the elderly and high-BMI individuals. The model shows good PK predictive performance that is generally better than existing models. When using this PK–PD model to target C_{e50}, propofol administration matches well with recommendations for anaesthesia in children, adults, elderly, and obese individuals. Targeting C_{e10} results in propofol administration matching well with recommendations for MAC sedation. This promotes confidence that the final PK–PD model will be useful in clinical TCI applications. Prospective clinical evaluation is required to determine its safety and efficacy.

Authors' contributions

Study design: D.J.E., M.M.R.F.S., A.R.A.
Data analysis: D.J.E., M.M.R.F.S., P.C.
Writing of the manuscript: all authors.

Acknowledgements

This work is the result of efforts of many contributors. Much of the pharmacokinetic (PK) data were obtained from the Open TCI Initiative website (opentci.org) collected through the efforts of S. L. Shafer, (Stanford, CA, USA), C. F. Minto (Sydney, Australia), and T. W. Schnider (St Gallen, Switzerland), and the numerous researchers who contributed data sets. Open sharing of data has allowed the authors to build the model based on the immense work of planning the studies and collecting the data sets. In turn, the authors also share their complete analysed PK and pharmacodynamic data sets, and the NONMEM control streams containing the model code. The authors extend deep appreciation to all of the researchers, clinicians, patients, healthy volunteers, and others who directly and indirectly contributed. The authors hope that others can improve or extend their results, and either directly or indirectly benefit from their model development.

Appendix A. Supplementary data

Supplementary data related to this article can be found at https://doi.org/10.1016/j.bja.2018.01.018.

Declaration of interest

D.J.E. and P.C. have no interest declared. A.R.A. has performed paid consultancy work for Janssen Pharmaceuticals (Janssen Pharmaceutica NV, Beerse, Belgium), The Medicines Company (Parsippany, NJ, USA), and EVER Pharma (EverPharma, Unterach am Attersee, Austria) (payment to institution). He is an editorial board member and editor of the British Journal of Anaesthesia. He was not involved in the editorial process of this publication. The research group/department of M.M.R.F.S. received grants and funding from The Medicines Company, Masimo (Irvine, CA, USA), Fresenius (Bad Homburg, Germany), Dräger (Lübeck, Germany), Acacia Design (Maastricht, The Netherlands), and Medtronic (Dublin, Ireland). M.M.R.F.S. receives honoraria from The Medicines Company, Masimo, Fresenius, Baxter (Deerfield, IL, USA), Medtronic, and Demed Medical (Temse, Belgium). He is a senior editor for *Anesthesia & Analgesia*, and an editorial board member and Director of the *British Journal of Anaesthesia*. He was not involved in the editorial process of this publication.

Funding

Department of Anesthesiology, University of Groningen; University Medical Center Groningen, Groningen, The Netherlands

References

1. Struys MM, Sahinovic M, Lichtenbelt BJ, Vereecke HE, Absalom AR. Optimizing intravenous drug administration by applying pharmacokinetic/pharmacodynamic concepts. *Br J Anaesth* 2011; **107**: 38–47
2. Struys MM, De Smet T, Glen JI, Vereecke HE, Absalom AR, Schnider TW. The history of target-controlled infusion. *Anesth Analg* 2016; **122**: 56–69
3. Absalom AR, Glen JI, Zwart GJ, Schnider TW, Struys MM. Target-controlled infusion: a mature technology. *Anesth Analg* 2016; **122**: 70–8
4. Struys MMRF, Absalom A, Shafer SL. Intravenous drug delivery systems. In: Miller RD, editor. *Miller's Anesthesia*. Philadelphia, Pennsylvania: Elsevier (Churchill Livingstone); 2014. p. 919–57
5. Eleveld DJ, Proost JH, Cortínez LI, Absalom AR, Struys MM. A general purpose pharmacokinetic model for propofol. *Anesth Analg* 2014; **118**: 1221–37
6. Eleveld DJ, Proost JH, Vereecke H, et al. An allometric model of remifentanil pharmacokinetics and pharmacodynamics. *Anesthesiology* 2017; **126**: 1005–18
7. Kim TK, Obara S, Egan TD. Disposition of remifentanil in obesity: a new pharmacokinetic model incorporating the influence of body mass. *Anesthesiology* 2017; **126**: 1019–32
8. Enlund M. TCI: target controlled infusion, or totally confused infusion? Call for an optimised population based pharmacokinetic model for propofol. *Ups J Med Sci* 2008; **113**: 161–70
9. R Core Team. *A language and envrionment for statistical computing*. Vienna, Austria: R foundation for Statistical Computing; 2015
10. Holford NH. A size standard for pharmacokinetics. *Clin Pharmacokinet* 1996; **30**: 329–32

11. Fisher DM, Shafer SL. Allometry, shallometry! *Anesth Analg* 2016; **122**: 1234–8
12. Kleiber M. Body size and metabolism. *Hilgardia* 1932; **6**: 315–53
13. West GB, Brown JH, Enquist BJ. A general model for the origin of allometric scaling laws in biology. *Science* 1997; **276**: 122–6
14. Anderson BJ, Holford NH. Mechanism-based concepts of size and maturity in pharmacokinetics. *Annu Rev Pharmacol Toxicol* 2008; **48**: 303–32
15. Al-Sallami HS, Goulding A, Grant A, Taylor R, Holford N, Duffull SB. Prediction of fat-free mass in children. *Clin Pharmacokinet* 2015; **54**: 1169–78
16. Zhang L, Beal SL, Sheinerz LB. Simultaneous vs. sequential analysis for population PK/PD data I: best-case performance. *J Pharmacokinet Pharmacodyn* 2003; **30**: 387–404
17. Zhang L, Beal SL, Sheinerz LB. Simultaneous vs. sequential analysis for population PK/PD data II: robustness of methods. *J Pharmacokinet Pharmacodyn* 2003; **30**: 405–16
18. Masui K, Upton RN, Doufas AG, et al. The performance of compartmental and physiologically based recirculatory pharmacokinetic models for propofol: a comparison using bolus, continuous, and target-controlled infusion data. *Anesth Analg* 2010; **111**: 368–79
19. Varvel JR, Donoho DL, Shafer SL. Measuring the predictive performance of computer-controlled infusion pumps. *J Pharmacokinet Biopharm* 1992; **20**: 63–94
20. Schüttler J, Kloos S, Schwilden H, Stoeckel H. Total intravenous anaesthesia with propofol and alfentanil by computer-assisted infusion. *Anaesthesia* 1988; **43**: 2–7
21. Glass PS, Shafer S, Reves JG. Intravenous drug delivery systems. In: Miller RD, editor. *Miller's Anesthesia*. Philadelphia, Pennsylvania: Elsevier (Churchill Livingstone); 2005. p. 439–80
22. Schnider TW, Minto CF, Gambus PL, et al. The influence of method of administration and covariates on the pharmacokinetics of propofol in adult volunteers. *Anesthesiology* 1998; **88**: 1170–82
23. Marsh B, White M, Morton N, Kenny GN. Pharmacokinetic model driven infusion of propofol in children. *Br J Anaesth* 1991; **67**: 41–8
24. Cortínez LI, Anderson BJ, Penna A, et al. Influence of obesity on propofol pharmacokinetics: derivation of a pharmacokinetic model. *Br J Anaesth* 2010; **105**: 448–56
25. White M, Kenny GN, Schraag S. Use of target controlled infusion to derive age and gender covariates for propofol clearance. *Clin Pharmacokinet* 2008; **47**: 119–27
26. Kataria BK, Ved SA, Nicodemus HF, et al. The pharmacokinetics of propofol in children using three different data analysis approaches. *Anesthesiology* 1994; **80**: 104–22
27. Short TG, Aun CS, Tan P, Wong J, Tam YH, Oh TE. A prospective evaluation of pharmacokinetic model controlled infusion of propofol in paediatric patients. *Br J Anaesth* 1994; **72**: 302–6
28. Rigby-Jones AE, Nolan JA, Priston MJ, Wright PM, Sneyd JR, Wolf AR. Pharmacokinetics of propofol infusions in critically ill neonates, infants, and children in an intensive care unit. *Anesthesiology* 2002; **97**: 1393–400
29. Rigby-Jones A, Priston M, Wolf A, Sneyd J. Paediatric propofol pharmacokinetics: a multicentre study. *Paediatr Anaesth* 2007; **17**: 610
30. Absalom A, Amutike D, Lal A, White M, Kenny GN. Accuracy of the 'Paedfusor' in children undergoing cardiac surgery or catheterization. *Br J Anaesth* 2003; **91**: 507–13
31. Absalom A, Kenny G. 'Paedfusor' pharmacokinetic data set. *Br J Anaesth* 2005; **95**: 110
32. Available from https://www.accessdata.fda.gov/drugsatfda_docs/label/2017/019627s066lbl.pdf (accessed 27 September 2017)
33. Glen JB. The development of 'Diprifusor': a TCI system for propofol. *Anaesthesia* 1998; **53**: 13–21
34. Servin F, Farinotti R, Haberer JP, Desmonts JM. Propofol infusion for maintenance of anesthesia in morbidly obese patients receiving nitrous oxide. A clinical and pharmacokinetic study. *Anesthesiology* 1993; **78**: 657–65
35. Anderson BJ, Holford NH. Mechanistic basis of using body size and maturation to predict clearance in humans. *Drug Metab Pharmacokinet* 2009; **24**: 25–36
36. Henthorn TK, Krejcie TC, Avram MJ. Early drug distribution: a generally neglected aspect of pharmacokinetics of particular relevance to intravenously administered anesthetic agents. *Clin Pharmacol Ther* 2008; **84**: 18–22
37. Doufas AG, Bakhshandeh M, Bjorksten AR, Shafer SL, Sessler DI. Induction speed is not a determinant of propofol pharmacodynamics. *Anesthesiology* 2004; **101**: 1112–21
38. Cortínez LI, De la Fuente N, Eleveld DJ, et al. Performance of propofol target-controlled infusion models in the obese: pharmacokinetic and pharmacodynamic analysis. *Anesth Analg* 2014; **119**: 302–10
39. Coppens MJ, Eleveld DJ, Proost JH, et al. An evaluation of using population pharmacokinetic models to estimate pharmacodynamic parameters for propofol and bispectral index in children. *Anesthesiology* 2011; **115**: 83–93
40. Chidambaran V, Venkatasubramanian R, Sadhasivam S, et al. Population pharmacokinetic–pharmacodynamic modeling and dosing simulation of propofol maintenance anesthesia in severely obese adolescents. *Pediatr Anesth* 2015; **25**: 911–23
41. Vuyk J, Lichtenbelt BJ, Olofsen E, van Kleef JW, Dahan A. Mixed-effects modeling of the influence of midazolam on propofol pharmacokinetics. *Anesth Analg* 2009; **108**: 1522–30
42. Hannivoort LN, Vereecke HE, Proost JH, et al. Probability to tolerate laryngoscopy and noxious stimulation response index as general indicators of the anaesthetic potency of sevoflurane, propofol, and remifentanil. *Br J Anaesth* 2016; **116**: 624–31
43. Bouillon TW, Bruhn J, Radulescu L, et al. Pharmacodynamic interaction between propofol and remifentanil regarding hypnosis, tolerance of laryngoscopy, bispectral index, and electroencephalographic approximate entropy. *Anesthesiology* 2004; **100**: 1353–72
44. Manyam SC, Gupta DK, Johnson KB, et al. When is a bispectral index of 60 too low? Rational processed electroencephalographic targets are dependent on the sedative–opioid ratio. *Anesthesiology* 2007; **106**: 472–83

45. Allegaert K, Hoon JD, Verbesselt R, Naulaers G, Murat I. Maturational pharmacokinetics of single intravenous bolus of propofol. *Pediatr Anesth* 2007; **17**: 1028–34
46. Kyle UG, Earthman CP, Pichard C, Coss-Bu JA. Body composition during growth in children: limitations and perspectives of bioelectrical impedance analysis. *Eur J Clin Nutr* 2015; **69**: 1298
47. Absalom AR, Mani V, De Smet T, Struys MM. Pharmacokinetic models for propofol—defining and illuminating the devil in the detail. *Br J Anaesth* 2009; **103**: 26–37
48. Anderson BJ, Holford NH, Woollard GA, Chan PL. Paracetamol plasma and cerebrospinal fluid pharmacokinetics in children. *Br J Clin Pharmacol* 1998; **46**: 237–43

Handling editor: H.C. Hemmings Jr